

Atomic layer deposition of an Al₂O₃ dielectric on ultrathin graphite by using electron beam irradiation*

Jiang Ran(蒋然)^{1,†}, Meng Lingguo(孟令国)¹, Zhang Xijian(张锡健)¹, Hyung-Suk Jung², and Cheol Seong Hwang²

¹School of Physics, Shandong University, Jinan 250100, China

²Department of Materials Science and Engineering, Seoul National University, Seoul 151-747, Korea

Abstract: Atomic layer deposition of an Al₂O₃ dielectric on ultrathin graphite is studied in order to investigate the integration of a high k dielectric with graphite-based substrates. Electron beam irradiation on the graphite surface is followed by a standard atomic layer deposition of Al₂O₃. Improvement of the Al₂O₃ layer deposition morphology was observed when using this radiation exposure on graphite. This result may be attributed to the amorphous change of the graphite layers during electron beam irradiation.

Key words: Al₂O₃; high k ; atomic layer deposition; graphene

DOI: 10.1088/1674-4926/33/9/093004

PACC: 7340; 7360H

1. Introduction

Graphene, a single layer of carbon atoms in a hexagonal lattice, has been studied intensively since its successful experimental isolation in 2004 due to its unique electrical and physical properties^[1]. Its extraordinarily high room temperature carrier mobility, combined with superior thermodynamic and mechanical properties, makes it a promising candidate for nano-electronic devices beyond the end of the Si-complementary metal-oxide semiconductor roadmap^[2,3]. For these graphene-based devices, a fine integration between graphene with the ultrathin high- k dielectrics is needed considering their future important roles to replace the traditional Si and Si oxide, respectively, in CMOS devices^[4–6].

Atomic layer deposition (ALD) is a thin film deposition technique that is based on the sequential use of a gas phase chemical process. The majority of ALD reactions use two chemicals (typically called precursors). These precursors react with a surface one at a time in a sequential manner. By exposing the precursors to the growth surface repeatedly, an ultrathin film (min. several atomic layer thickness) can be deposited. ALD is the most extensively utilized deposition technique for growing high- k gate dielectric layers, and it shows significant advantages for fabricating ultrathin (< 10 nm) film as compared with many other deposition methods^[7,8]. However, the deposition of high- k dielectric layers on ultrathin graphite using the ALD technique has been relatively limited due to the hydrophobic and inert nature of the graphite basal plane^[9–11]. The deposition morphology of the ALD dielectric layer on a clean graphite surface is a striated growth at the steps between graphite layers^[12]. Recently, some chemical pretreatments of the graphite surface using NO₂, organic acid or O₃, have been proposed to improve the ALD growth of high- k dielectrics^[13,14]. Here we present the observation

of the improved growth morphology of ALD-deposited Al₂O₃ on a highly oriented pyrolytic graphite (HOPG) surface after electron beam (e-beam) irradiation, which shows a terraced morphology instead of the characteristic selective and striated one on common graphite. The results suggest that thin uniform high- k films might be achieved with the help of e-beam irradiation by an increase in nucleation sites on the basal planes.

2. Experimental details

Prior to the Al₂O₃ layer growth by ALD, the crystals of graphite are obtained by mechanical exfoliation from bulk HOPG using adhesive tape. Two treatments, i.e., vacuum annealing and electron beam irradiation, were then applied to the HOPG samples. The vacuum anneal is performed at 500 °C for 30 min to remove any physisorbed species, such as H₂O or other compounds. The irradiation time ranges from zero to 35 min. An XL30 ESEM-TMP scanning system (Holland Philips-FEI Company) with a tungsten electron gun was used to provide electron beam irradiation. The working distance for the samples is ~8 mm away from the tip of the electron gun, with the accelerating voltage fixed as 24 kV (adjustable 1–30 kV). The working area is ~2 × 10⁹ nm² under the continuous electron beam with the corresponding beam current at ~1.8 × 10⁻¹⁰ A. The flux has been fixed for each sample in experiments in order to guarantee that the electron dose is proportional to the irradiation time.

Based on the above HOPG pretreatment, Al₂O₃ layers in 50–200 cycles were then deposited on top of the HOPG at 200 °C with trimethylaluminum (TMA) and H₂O as reactants. For selected samples, O₃ was also used as an oxidant for comparison. A commercial ALD reactor (Genitech, Inc., prototype) was used to grow the Al₂O₃ films. Nitrogen was used as a carrier and purge gas. One ALD cycle was per-

* Project supported by the Independent Innovation Foundation of Shandong University, China (No. 2010TS023), the China Postdoctoral Special Foundation (No. 200902556), the China Postdoctoral Science Foundation (No. 20080431176), and the Postdoctoral Innovation Foundation of Shandong Province, China (No. 200702027).

† Corresponding author. Email: jiangran@sdu.edu.cn

Received 22 November 2011, revised manuscript received 28 May 2012

© 2012 Chinese Institute of Electronics

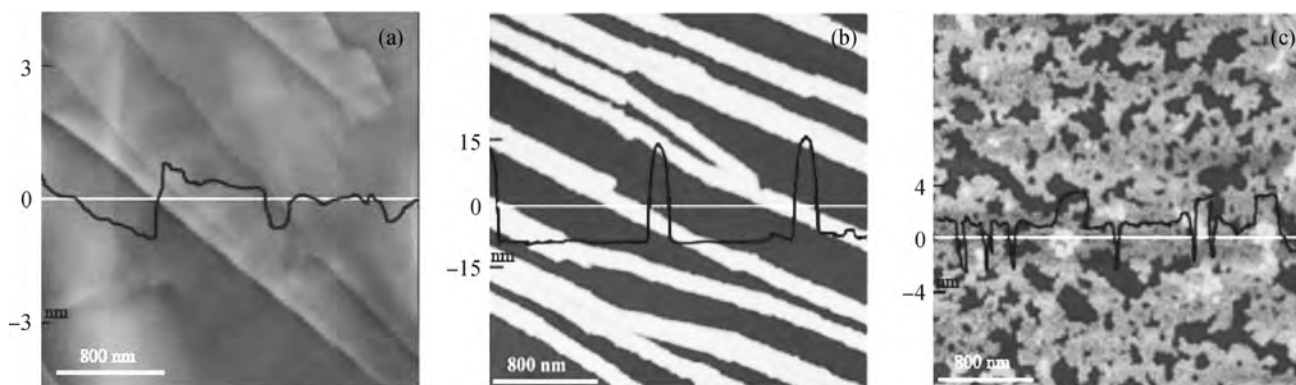


Fig. 1. AFM images of (a) a typical fresh HOPG surface and (b) Al_2O_3 layer deposited on the HOPG surface which underwent 35 min irradiation (200 cycles). This step-edge growth morphology is similar to the HOPG surface without irradiation (not shown). (c) The Al_2O_3 layer deposited on the HOPG surface under 5 min irradiation (50 cycles).

formed using the following sequence: TMA (3 s)– N_2 purge (5 s)– $\text{H}_2\text{O}/\text{O}_3$ (2 s)– N_2 purge (5 s). During the ALD process, the TMA precursor and the substrate were kept at 85 °C and 200 °C, respectively. The deposited Al_2O_3 layers and corresponding HOPG were characterized by using atomic force microscopy (AFM), Raman spectroscopy, and X-ray photoelectron spectroscopy (XPS), respectively.

3. Results and discussion

Figure 1(a) shows the AFM morphology image of a typical fresh HOPG surface, which possesses smooth basal planes and obvious step edges. Figure 1(b) illustrates the morphology image of the 35-min-irradiation HOPG surface on which the Al_2O_3 layer was deposited by ALD with 200 cycles of TMA/ H_2O process. The HOPG surface without irradiation also shows the same kind of step-edge growth morphology. It can be concluded that sufficient long-time (35 min) irradiation has no obvious influence on the Al_2O_3 coverage on HOPG, as reported^[12]. The Al_2O_3 layer was formed only along the step edges and not on the inert basal planes if the HOPG did not undergo any pretreatment. This striated growth of Al_2O_3 is commonly interpreted by the one dimensional nucleation site at step edges^[12], since the key factor enabling the high- k dielectric layer growth on graphite by ALD is the presence of nucleation sites on the inert surface of graphite^[15, 16]. Interestingly, the Al_2O_3 layer deposited on the HOPG surface with much shorter irradiation time, as shown in Fig. 1(c), can be formed on the basal planes except for the step edges, though the growth does not totally cover the HOPG surface. It is noted that the Al_2O_3 layer on the irradiated HOPG surface is not uniform except for the uncovered region, which is probably due to the topography-induced growth-speed difference between the basal planes with the step edges. The brightest striated regions in Fig. 1(c) could be the Al_2O_3 layers which fitly grow on the step edges, where high k is most easily accumulated, as mentioned above.

The morphology of the 35 min irradiated sample is the same as the un-irradiated one, but the sample with 5 min irradiation shows wider coverage. It is naturally expected that the irradiation time has a severe influence on the HOPG surface, as shown in Fig. 2. One can find that the ratio climbs quickly

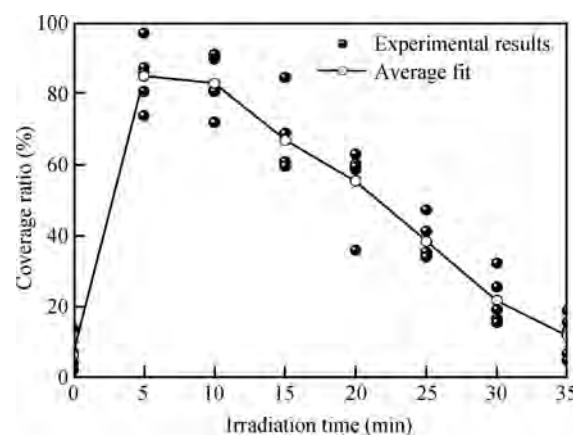


Fig. 2. Coverage ratios of Al_2O_3 layers on the HOPG substrates with various irradiation times from 0 to 35 min. The open circle denotes the corresponding average value.

during the initial short time, and then falls gradually. This observation strongly proves that the improved Al_2O_3 coverage on the basal planes of HOPG is related to the e-beam irradiation, which leads to a dynamic change of the thin graphite. We have investigated all of the samples, and concluded that ~5 min is the maximum point, though there is slight difference for each sample.

In order to verify the influence of e-beam irradiation time on the HOPG, Raman spectra of HOPG substrates with various-time irradiation were investigated, as shown in Fig. 3. For comparison, Raman spectrum of fresh HOPG was also present. There are only two intense features in the spectra for the fresh HOPG sample, which are the in-plane vibrational G band and the two phonon 2D band, respectively. There is no D band present in the fresh HOPG and the corresponding G band is smaller than that of irradiated samples. These results confirm the perfect crystal properties of the unirradiated HOPG sample.

A clear difference between the HOPG substrates before and after irradiation is that a strong D peak located at 1346 cm^{-1} occurs after irradiation. This Raman band is a disorder-induced band, which is activated by a double resonance effect by defects, such as in-plane substitutional heteroatoms, vacancies, or grain boundaries^[17, 18]. The “substitu-

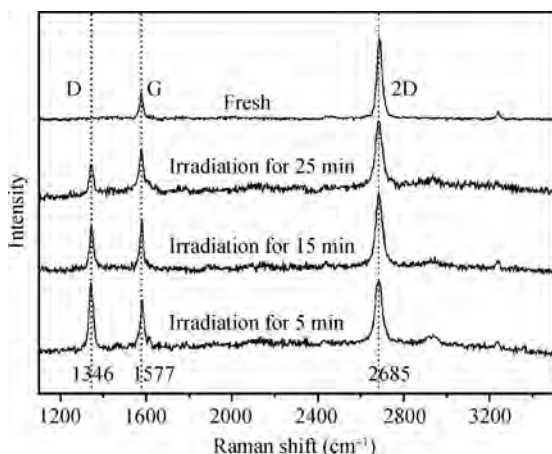


Fig. 3. Raman spectra of HOPG substrates with various irradiation times before Al_2O_3 deposition. The unirradiated fresh graphite is also shown for comparison. The D band intensity decreases with the increase of irradiation time but is invisible for fresh graphite. It shows little difference between the sample for the Raman spectra, regardless of whether vacuum annealing or irradiation is applied first, and the only slight difference is the intensity difference of D band. This figure is the sample with “irradiation + annealing” treatment.

tional hetero-atoms and vacancies” defects could be ascribed to the surface species (such as hydroxyl) during electron beam irradiation. The “grain boundaries” should be due to the amorphous effect of irradiation on HOPG.

Meanwhile, another obvious observation in Fig. 3 is that the intensity of the D band decreases with irradiation time after 5 min. This can be understood as being due to the amorphous evolution (the reduction of grain boundaries) during the e-beam irradiation. It is noted that the evolution tendency of the D band intensity with irradiation time is consistent with that of Al_2O_3 coverage on HOPG (Fig. 2). Therefore, it is feasible to deduce that the nanocrystals and the corresponding boundaries, as nucleation sites, could be highly related to the improved Al_2O_3 coverage on HOPG. Meanwhile, from Fig. 1(c), the morphology of Al_2O_3 also seems like nanocrystal units accumulating together.

As shown in Fig. 4, the original HOPG crystal may be scattered to nanocrystals rapidly once irradiation is applied. With further irradiation, the HOPG is so disordered that the nanocrystals further evolve to be in an amorphous state. During this process, the nucleation sites are decreased due to the reduction of nanocrystal clusters. Therefore, the Al_2O_3 coverage ratio on HOPG is decreased with increasing the irradiation time. The function of the HOPG nanocrystals is somewhat similar to a previous study of evaporated Al on highly oriented pyrolytic graphite surfaces^[9], where the deposited nanoscale Al crystals are also found as the nucleation point in Al_2O_3 deposition.

The e-beam irradiation belongs to a physical treatment, which is different to the chemical ones on HOPG, such as using NO_2 and O_3 reactive with graphite. Therefore, it could be an advantage for this simple method that there is no new element (N) introduction compared with the NO_2 pretreatment method. However, it seems that there is no introduction of a new element onto HOPG by using the chemical pretreatment

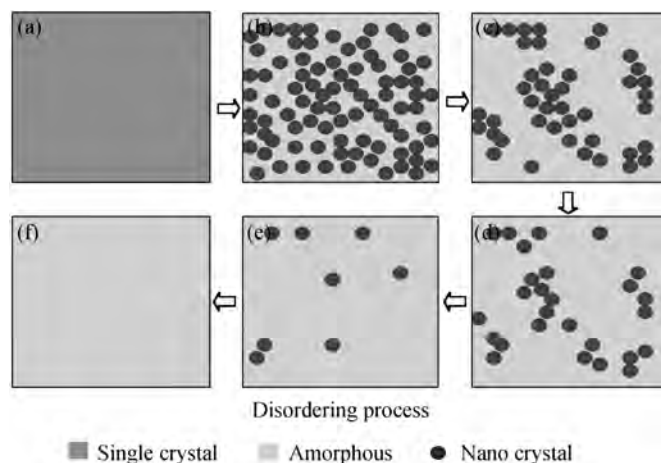


Fig. 4. Cursory schematic diagram for the disordering process of HOPG due to e-beam irradiation. The original crystal is scattered to nanocrystals and then further evolves to be in an amorphous phase.

of O_3 , since oxygen will be finally introduced during the high k (Al_2O_3) deposition. It is necessary to understand the comparative influences of irradiation/ O_3 treatment on the ALD integration of a dielectric layer with HOPG in order to understand the characteristic of the irradiation treatment. As shown in Fig. 5, the XPS spectra of the ALD deposited Al_2O_3 on an irradiated HOPG surface is presented relative to on O_3 -treated graphite ones.

The $\text{O}1s$ spectrum of the O_3 treated sample shows a wider FWHM in contrast to the sample with irradiation treatment. This result proves the strong oxidation ability of O_3 and indicates that more oxide components are formed due to the intense O_3 oxidation. Both $\text{O}1s$ lines are mainly located at 531.4 eV, which is consistent with the fully oxidized Al–O bond^[19]. This is confirmed by the corresponding $\text{Al}2p$ lines shown in Fig. 4(b), which consist of a fully oxidation Al–O bonding peak centered at about 74.8 eV and no Al–C bond was observed for both samples. Considering the fine oxidation of Al, the observation of the obvious $\text{O}1s$ extending for the sample with O_3 treatment is probably due to the formation of C oxide species. As shown in Fig. 4(c), The $\text{C}1s$ spectrum of the sample with O_3 treated HOPG extends to higher energy compared to that with irradiation treated sample. An intense subpeak at about 285.3 eV is present for the O_3 treated sample, which is known as the C–O–C epoxide bonding. Therefore, the O_3 treatment could cause carbon bonding scission and oxidation. Due to the lattice disordering as mentioned above, the $\text{O}1s$ and $\text{C}1s$ lines of the irradiation-treated sample also extend to higher bonding energy and the line shapes are not in perfect symmetry, but it is much slighter than that of the O_3 -treated sample. Most importantly, we have not observed the obvious C scission behavior under the accuracy of the XPS detection, which is believed to be an advantage over to the O_3 treatment process. However, considering the nonuniformity of the Al_2O_3 coverage on HOPG, the O_3 treatment method shows its own advantage as a chemical method. Therefore, it is hard to state which process is superior, but with different characteristics. Further understanding of the e-beam irradiation on high k deposition on HOPG is ongoing.

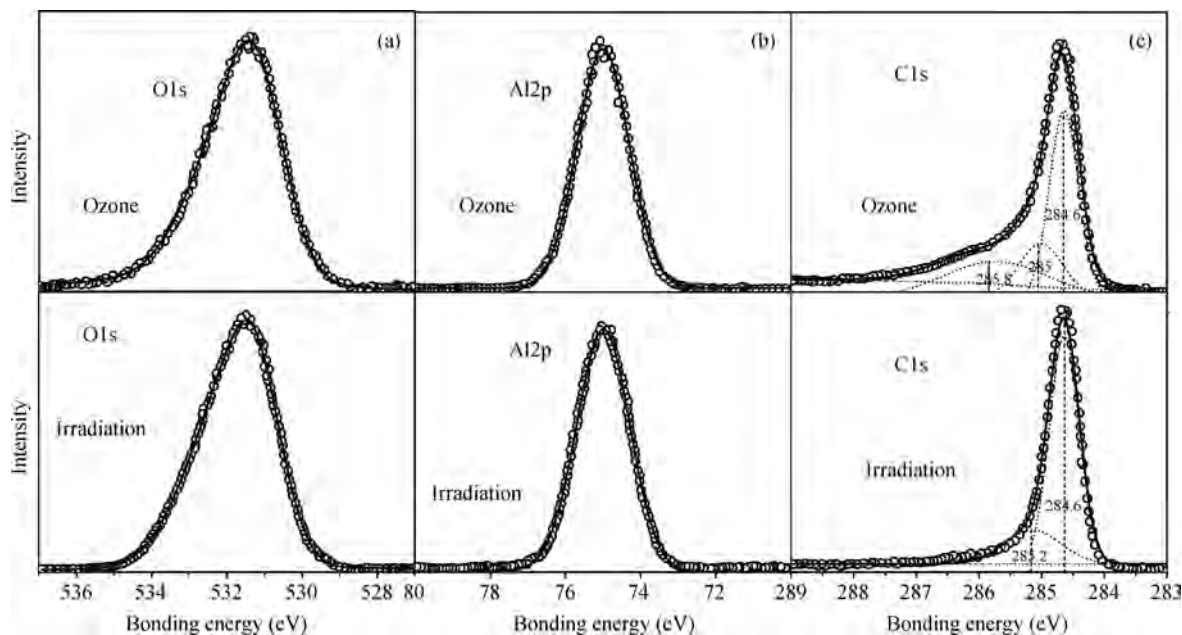


Fig. 5. O1s, Al2p and C1s spectra of Al_2O_3 deposited on the HOPG treated by ozone and irradiation, respectively.

4. Conclusion

In summary, the improved ALD fabrication of an Al_2O_3 dielectric on HOPG due to e-beam irradiation is presented. The irradiation will not introduce unnecessary impurities on the HOPG surface. It is preliminary deduced that the improvement Al_2O_3 deposition is highly related to the disordering evolution of HOPG under e-beam irradiation. The treatment of e-beam irradiation on HOPG followed by ALD fabrication may add new knowledge on the combination of a high k dielectric with a graphite substrate.

References

- [1] Novoselov K S, Geim A K, Morozov S V, et al. Electric field effect in atomically thin carbon films. *Science*, 2004, 306(5296): 666
- [2] Stankovich S, Dikin D A, Dommett G H B, et al. Graphene-based composite materials. *Nature (London)*, 2006, 442: 282
- [3] Ghosh S, Calizo I, Teweldebrhan D, et al. Extremely high thermal conductivity of graphene: prospects for thermal management applications in nanoelectronic circuits. *Appl Phys Lett*, 2008, 92(15): 151911
- [4] Neto A H C, Guinea F, Peres N M R, et al. The electronic properties of graphene. *Rev Mod Phys*, 2009, 81(1): 109
- [5] Wilk G D, Wallace R M, Anthony J M. High- k gate dielectrics: current status and materials properties considerations. *J Appl Phys*, 2001, 89(10): 5243
- [6] Nam S, Nam S W, Yoo J H, et al. Interface control by modified sputtering on Pt/HfO₂/Si system. *Mater Sci Eng B*, 2003, 102(1): 123
- [7] Deshpande A, Inman R, Jursich G, et al. Characterization of hafnium oxide grown on silicon by atomic layer deposition: interface structure. *Microelectron Eng*, 2006, 83(3): 547
- [8] Vainonen-Ahlgren E, Tois E, Ahlgren T, et al. Atomic layer deposition of hafnium and zirconium silicate thin films. *Computational Materials Science*, 2003, 27(1/2): 65
- [9] Pirkle A, Wallace R M, Colombo L. *In situ* studies of Al_2O_3 and HfO_2 dielectrics on graphite. *Appl Phys Lett*, 2009, 95(13): 133106
- [10] Lee B, Park S Y, Kim H C, et al. Conformal Al_2O_3 dielectric layer deposited by atomic layer deposition for graphene-based nanoelectronics. *Appl Phys Lett*, 2008, 92(20): 203102
- [11] Yang H F, Yang R T. *Ab initio* molecular orbital study of adsorption of atomic hydrogen on graphite: insight into hydrogen storage in carbon nanotubes. *Carbon*, 2002, 40(3): 437
- [12] Xuan Y, Wu Y Q, Shen T, et al. Atomic-layer-deposited nanostructures for graphene-based nanoelectronics. *Appl Phys Lett*, 2008, 92(1): 013101
- [13] Wang X, Tabakman S M, Dai H. Atomic layer deposition of metal oxides on pristine and functionalized graphene. *J Am Chem Soc*, 2008, 130(26): 8152
- [14] Lin Y M, Jenkins K A, Valdes-Garcia A, et al. Operation of graphene transistors at gigahertz frequencies. *Nano Lett*, 2009, 9(1): 422
- [15] Liang X, Zhan G, King D M, et al. Alumina atomic layer deposition nanocoatings on primary diamond particles using a fluidized bed reactor. *Diamond & Related Materials*, 2008, 17(2): 185
- [16] Farmer D B, Gordon R G. Atomic layer deposition on suspended single-walled carbon nanotubes via gas-phase noncovalent functionalization. *Nano Lett*, 2006, 6(4): 699
- [17] Thomsen C, Reich S. Double resonant Raman scattering in graphite. *Phys Rev Lett*, 2000, 85(24): 5214
- [18] Baranov A V, Bekhterev A N, Bobovich Y S, et al. Interpretation of certain characteristics in Raman spectra of graphite and glassy carbon. *Optics and Spectroscopy*, 1987, 62: 5
- [19] Renault O, Gosset L G, Rouchon D, et al. Angle-resolved X-ray photoelectron spectroscopy of ultrathin Al_2O_3 films grown by atomic layer deposition. *J Vac Sci Technol A*, 2002, 20(6): 1867